

Bio-polyols synthesized by liquefaction of cellulose: influence of liquefaction solvent molecular weight

Adam Olszewski^{1*}, Paulina Kosmela¹, Łukasz Piszczyk¹,

¹Department of Polymer Technology, Chemical Faculty, G. Narutowicza St. 11/12, Gdansk University of Technology, 80-233 Gdansk, Poland; Adam.Olszewski@pg.edu.pl (A.O.)

Orcid: 0000-0002-6866-4933; Paulina.Kosmela@pg.edu.pl (P.K.) Orcid: 0000-0003-4158-2679, Lukasz.Piszczyk@pg.edu.pl (Ł.P) Orcid: 0000-0003-1363-4988

* Correspondence: Adam.Olszewski@pg.edu.pl;

Abstract

Currently, the plastics industry including polyurethanes is based on the use of petrochemicals. For this reason, scientists are looking for new types of renewable resources for the substitution of petrochemical substances. This work aims to evaluate the effect of polyethylene glycols (PEG) with different molecular mass impact on properties of bio-based polyols synthesized via biomass liquefaction of cellulose. To date, research has mostly focused on the use of different biomass sources, but the area of bio-polyols synthesis with PEG with various molecular weights has not been explored in depth. For this reason, polyols were synthesized using PEG with a molecular weight in the range of 200–600 g/mol. Depending on the type of liquefaction solvent, the bio-polyols showed a hydroxyl value of 519–652 mgKOH/g, a viscosity of 0.736–1.415 Pa·s, and a water content below 1%. Observed difference may be related to change of reactivity of the PEG chains caused by steric hindrance of longer chains and the difference in the amount of reactive OH groups. These findings add substantially to understanding of the influence of liquefaction solvent molecular mass on the properties of new bio-polyols and those of polyurethane materials.

Keywords: Polyol, biomass liquefaction, cellulose, polyethylene glycol,

1. Introduction

In recent decades, because of the increase in environmental awareness and noticeable environmental degradation, the area of ecology in polyurethane (PU) manufacturing has attracted increasing attention^{1,2}. Currently, for the manufacturing of the PU materials, manufacturers are mainly using large amounts of petroleum-based resources, such as isocyanates, polyester/polyether polyols, chain extenders, and additives^{3,4}. The large-scale use of petroleum-based resources is leading to the depletion of fossil resources, environmental pollution, and accelerated global warming. For these reasons, scientists are looking for new methods to replace petroleum-based resources in the polyurethane industry⁵. Among these methods, the most attention is given to the processing of natural substances into useful semi-products which can be used as substitute for petrochemical polyols. The most popular natural substances used in such processes is castor oil^{6,7}, soybean oil^{8,9}, rapeseed oil^{10,11}, mustard seed oil^{12,13}, cellulose^{14,15}, lignin^{16,17} or wood and its derivatives^{18–20}.

One of the commonly used processes for biomass transformation into polyols is the biomass liquefaction, which relies on cleavage of long biomass chains to low molecular valuable chemicals. This process can be divided to indirect liquefaction and solvent liquefaction²¹. The indirect liquefaction begins with the transformation of biomass into syngas, which is used for the synthesis of full-value products. A more interesting process in terms of the polyurethane industry is solvent liquefaction, which directly transforms biomass into liquids in the presence of proper liquefaction solvent and catalyst^{21,22}. The process of solvent liquefaction is also known as solvothermal liquefaction, because it is mainly conducted at elevated temperatures from 120 to 250 °C in normal pressure. This process is based on the

solvolysis reaction between biomass and polyhydric alcohols (liquefaction solvents) that causes the decomposition of the biomass structure⁵. The most important substances that are commonly used in this process include different purity glycerol and poly (ethylene glycol) (PEG) with different molecular mass²³. The described reaction takes place with the use of a catalyst. The most common catalysts used in this process include strong acids, including sulfuric acid^{24,25} and p-toluenesulfonic acid^{26,27}, strong bases, including sodium hydroxide^{28,29}, and ionic liquids. Due to the number of possible reactions between the reaction components, the resulting liquid product which may be called *bio-polyol* is a mixture of compounds rich in hydroxyl groups. The synthesized polyol is mainly composed of glycols, glycerol derivatives (e.g. condensed glycerols), ethers, carbohydrate derivatives, esters, acids, and water³⁰. Based on the scientific literature, the potential pathway of conducted reaction and examples of reaction products are presented in Fig. 1^{18,23,31}. Excess of water in the polyol composition may be removed by drying at elevated temperature with reduced pressure³². Moreover, in the literature, it is possible to find methods for separating bio-polyol into fractions due to the differences of solubility. These processes may allow for regeneration of used liquefaction solvents, and isolation of useful substances from solid residues such as cellulose nanofibers and nanocrystals³³.

Depending on the parameters of the synthesis, the composition of the reaction mixture and the treatment undergone, the bio-polyols can find a wide range of applications. Additionally, the properties of the obtained bio-polyols allow their use during the reaction injection molding (RIM) and reactive extrusion which can be a very interesting process for bio-based materials manufacturing. On the other hand, these processes require a process understanding, control of the temperature, stress and residence time distributions along the extruder^{34,35}. Bio-polyols are most commonly used as substitutes for petrochemical polyols in the manufacturing of polyurethane foams. Usually, the amount of bio-polyol in such foam's ranges from 10 to 30%, but it is possible to find research in which the authors prove that the addition of bio-polyol may be higher. Tran et al.³⁶ in their work provides a detailed description of the synthesis by liquefaction of macroalgae *Saccharina japonica*. The biomass liquefaction process was carried out in the mixture of crude glycerol and PEG300 and optimized by a change in catalyst loading, reaction time, and temperature. For the analysis of different reaction conditions author used response surface methodology and indicated that optimal reaction parameters are temperature of 160 °C, 4.25% catalyst loading, and time of 65 min. Synthesized polyol were used for the manufacturing of polyurethane foam. The PU formulation included 30% addition of bio-polyol. The impact of bio-polyol on polyurethane foam properties was investigated by thermogravimetric analysis, high-resolution scanning electron microscopy, and FTIR spectroscopy. The higher addition of bio-polyol during manufacturing of PU foams was proposed by Chang et al.³⁷. Authors synthesized foams with 100% content of bio-polyol from obtained by liquefaction of wheat straw in crude glycerol. In addition, the author used the addition of flame retardants to reduce the flammability of the manufactured materials. It should be emphasized that higher addition of bio-polyols may cause modification of foam structure and deterioration of mechanical properties and thermal conductivity of manufactured materials.

Polyurethane foams manufacturing is not the only application of bio-polyols. These substances may be used during the preparation of polyurethane adhesives. Jiang et al.³ offers a comprehensive review of the application of bio-polyol in wood adhesives. Juhaida et al.³⁸ in their research prepared bio-polyol by liquefaction of kenaf core and applied it in synthesis of polyurethane adhesive. Obtained adhesive was composed of synthesized bio-polyols: toluene-2,4-diisocyanate (TDI), 1,4-butanediol (BDO). As a catalyst of curing trimethylamine (TEA) was used. The authors tested glue bond integrity of the rubberwood laminates and assessed the quality of the bonding. It was observed that water present in bio-polyol caused generation of carbon dioxide (CO₂) during adhesive curing what was the main reason of poor bonding strength of adhesive.



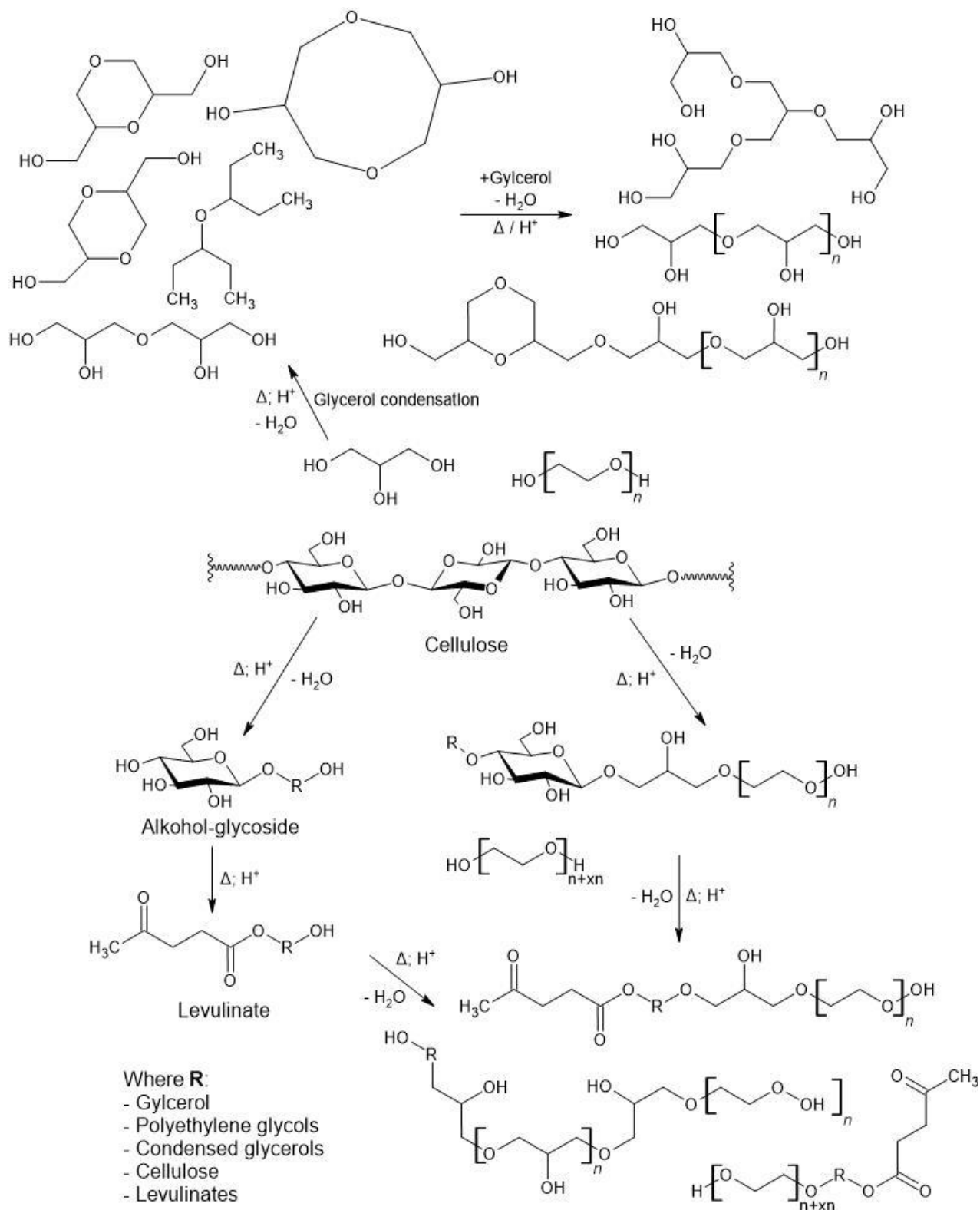


Figure 1. Possible reactions which may occur during the biomass liquefaction

Recent findings in development of materials with addition of bio-polyols have led to manufacturing of other types of polyurethane materials. These materials may include polyurethane resins¹⁸, superhydrophobic polyurethanes³⁹, materials for energy harvesting⁴⁰, shape memory materials⁴¹, composites with addition of inorganic⁴², and organic fillers^{43,44}. The most interesting of them may be polyurethane wood-composites, which may be alternative for commonly used polymer wood composites made of polyolefins. This approach was presented in our recent studies⁴⁵. In this paper, the authors demonstrated the preparation of bio-polyols by liquefaction of mixed wood wastes in three different liquefaction solvents. The temperature of the liquefaction process was 150 °C for 6 h. The obtained bio-polyols were characterized and used for the preparation of polyurethane materials. Manufactured materials were tested and the PU matrix with the best properties was used for the development of polyurethane wood composites (PU-WC). Composites with addition up to 70% of wood shavings were manufactured and tested.

Taking into account the scientific articles, it can be concluded that polyol synthesized via solvothermal liquefaction can be successfully used as substitution of petrochemical polyols in polyurethane materials. As the polyols have crucial impact on the performance of PU materials, the impact of reaction mixture should be investigated. The available scientific literature offers a comprehensive overview of the impact of different substances on polyol properties. The approaches used have failed to provide detailed information on the influence of the molecular weight of polyethylene glycol (PEG) on the properties of the synthesized polyol. The chain length of polyethylene glycol may influence the course of the reactions during biomass liquefaction which affect chemical structure of obtained polyols, total amount of hydroxyl groups, viscosity and biomass conversion degree. These parameters influence the soft segments and modify its structure and properties. Furthermore, the structure of the soft segment affects the interactions with rigid and formation of hydrogen bonds, which may decide about the degree of microphase separation⁴⁶.

As the properties of polyols have a huge impact on the properties of manufactured polyurethanes, this study aims to determine the influence of polyethylene glycols with different molecular mass on the course of biomass liquefaction process and bio-polyol properties. For this reason, biomass liquefaction of cellulose in the presence of glycerol and polyethylene glycols with different molecular mass (200 – 600 g/mol) were conducted. To control the course of the biomass liquefaction, a change of the hydroxyl value and biomass conversion was controlled. The obtained polyols were characterized by rheological studies and water content by Karl Fischer titration. To confirm the presence of significant functional groups, Fourier transform infrared spectroscopy (FTIR) was conducted. Moreover, the thermal stability of bio-polyols was determined by thermogravimetric analysis (TGA). Finally, the obtained bio-polyols were compared in terms of polyurethane materials manufacturing.

2. Experimental

2.1. Materials and characterization

The characteristics of used materials and details about their suppliers are presented in the subsection SD1 in Supplementary Data File (SDF). Furthermore, the detailed description of applied research techniques is explained in Subsection SD2. Briefly, the course of biomass liquefaction and properties of the final product were characterized by the hydroxyl value, biomass conversion degree, water content by Karl Fischer titration, rheological studies, Fourier transform infrared spectroscopy (FTIR), thermogravimetric analysis (TGA) and differential scanning calorimetry (DSC). All the listed research methods were performed in accordance with international standards (if applicable), and the test parameters and description of the apparatus were included in the Supplementary Data File.

2.2. Two-step preparation of bio-based polyols



The biomass liquefaction was carried out in the same way as in our previous studies^{15,43}. Two-step cellulose liquefaction was conducted under atmospheric pressure in a three-neck reactor. The reactor was placed inside the heating mantle and equipped with a thermometer, condenser, and mechanical stirrer. The liquefaction solvent (50/50% weight mixture of glycerol and polyethylene glycols with different molar masses – PEG 200/PEG400/PEG600) was poured into the reactor. As a catalyst, 3% by weight sulfuric acid (95% purity) was added. The mass ratio of cellulose to the liquefaction solvent was 1:10. The first step of the reaction was carried out at 150 °C for 6 hours. The mixture was stirred at 150 rpm. To determine the properties of bio-polyols, the samples of the polyol were collected every hour. During the second step, the mixture was neutralized with potassium hydroxide and dried under reduced pressure for 2 hours. The final product was poured into an airtight container and placed in a dark and cold place. The schematic representation of the process is shown in Fig. 2.

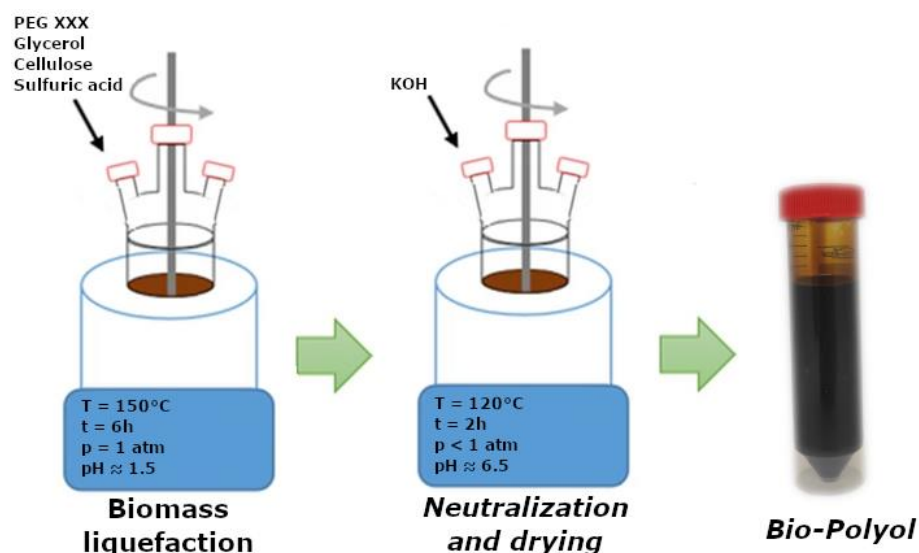


Figure 2. Schematic representation of the two-step preparation of bio-based polyols

3. Results and discussion

3.1. Physical properties

To investigate the course of the biomass liquefaction the hydroxyl value and biomass conversion were examined before heating and adding catalyst and every hour during the reaction (it was considered that reaction starts (t_0) when reaction mixture reaches 150 °C). The results of these tests are presented in Figs. 3. a) and b). The hydroxyl values of reagent mixtures and the final properties of polyols after neutralization and drying are presented in Table 1. As can be seen at Fig. 3a. the most significant change of hydroxyl value at first 3 hours of reaction can be notice for sample P_200 and P_400. This may be due to the higher amount of hydroxyl groups in the mixture which can undergo a reaction. For sample P_600, the presence of glycols with higher molecular masses causes higher viscosity of the system and causes possible steric hindrances. For these reasons, the reaction of biomass liquefaction may be slower. Moreover, the water content of the polyol has a significant impact on the hydroxyl value. During the process, water particles are the main by-product of the reaction. These particles affect the actual hydroxyl value, what may be particularly important for samples with a higher content of hydroxyl groups in the mixture of solvents. In addition, a temporary increase in the hydroxyl value during the reaction may be caused by the higher water content. This is especially

noticeable for longer reaction times when the viscosity of the mixture is higher and collecting of the by-product is more difficult. The hydroxyl value of synthesized polyols after neutralization and drying suggests the possible application of polyols in the production of rigid polyurethane foams and was 652 ± 26 ; 519 ± 20 ; 589 ± 19 mg KOH/g, for P_200, P_400 and P_600, respectively. The hydroxyl value of bio-polyols does not decrease in a monotonic manner, due to the abovementioned effects of reduced reactivity of samples with higher viscosity and higher water content.

Analyzing the degree of biomass conversion, it can be noticed that all liquefaction solvent mixtures provided over 90% biomass conversion at the end of reaction. The highest biomass conversion was noted for sample P_200 (BC = 94.3 ± 1.6 %). It may be due to a more intensive process of biomass transformation due to the reaction with shorter PEG chains. On the other hand, the sample coded P_600 (BC = 90.9 ± 1.1 %) sample is characterized by the lowest biomass conversion, which may be caused by the more intense formation of particles with a higher molecular weight or repolymerization of decomposition products into xylosides and glucosides⁴⁷.

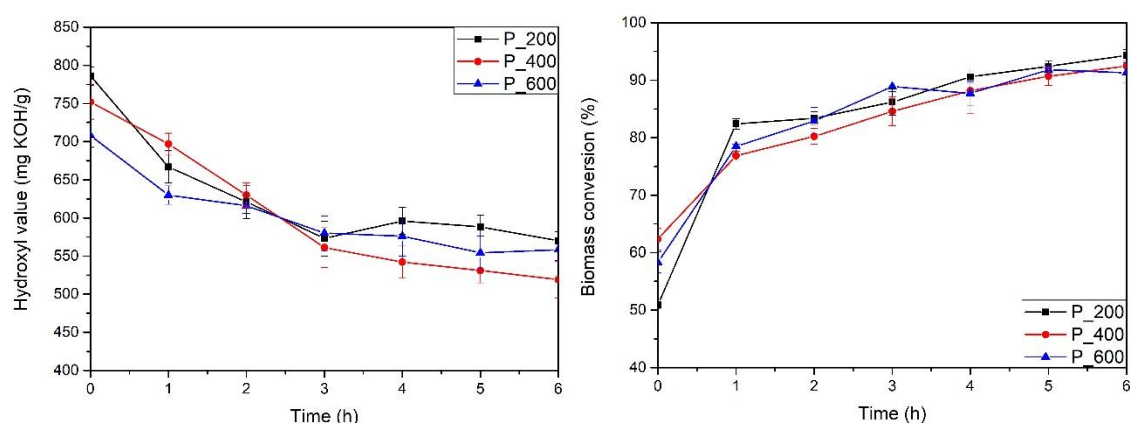


Figure 3. Hydroxyl value (a) degree of biomass conversion (b) of bio-polyols

Table 1. The hydroxyl value before heating and the final properties of the obtained polyols after neutralization and drying

| Sample | Hydroxyl value before heating [mg KOH/g] | Hydroxyl value after neutralization [mg KOH/g] | Biomass conversion [%] | Viscosity [Pa·s] | | Water content [%] |
|--------|--|--|------------------------|------------------|-------|-------------------|
| | | | | 30 °C | 50 °C | |
| P_200 | 926 ± 31 | 652 ± 26 | 94.3 ± 1.6 | 0.736 | 0.187 | 0.82 ± 0.11 |
| P_400 | 781 ± 18 | 519 ± 20 | 91.4 ± 0.8 | 0.790 | 0.195 | 0.67 ± 0.04 |
| P_600 | 751 ± 23 | 589 ± 19 | 90.9 ± 1.1 | 1.415 | 0.359 | 0.64 ± 0.09 |

3.2. Rheological properties

As the viscosity is a crucial parameter for the further application of biopolyols in the manufacturing of polyurethane materials, the rheological properties were tested at two temperatures $T_1 = 30$ °C and $T_2 = 50$ °C. The results of this study are shown in Fig. 4. and Fig. 5. The analysis using the study results of the Herschel-Bulkley model is presented in Table 2.

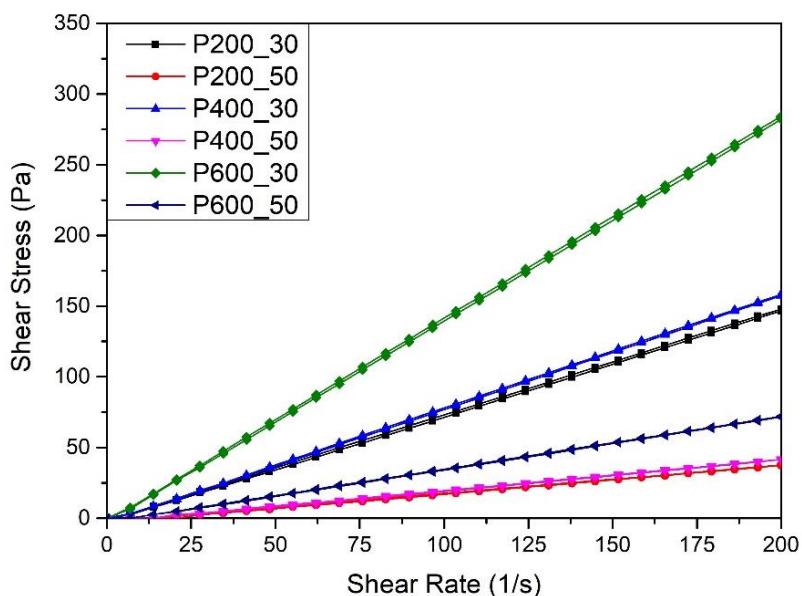


Figure 4. The flow curves in different temperatures of synthesized polyols

Analyzing course of flow and viscosity curves for all polyols it can be noticed that the shear stress and viscosity decrease with increasing temperature of measurement. This effect may be due to the supply of energy to the system, which increased macromolecules mobility and changed the intermolecular spacing⁴⁸. The maximal value of shear stress was observed for polyol samples at $T_1 = 30\text{ }^\circ\text{C}$. The shear stress and viscosity at T_1 is the highest for polyol P_600 ($\tau = 272\text{ Pa}$), what may be caused by higher viscosity of used PEG 600. Moreover, it can be observed that the shear stress and viscosity of P_200 ($\tau = 149\text{ Pa}$) and P_400 ($\tau = 142\text{ Pa}$) polyol are comparable. This effect may be caused by higher degree of reaction of the components with shorter chains of PEG and reduced viscosity of such compounds. At $T_2 = 50\text{ }^\circ\text{C}$ the shear stress of all polyols was reduced significantly to 53, 28, 25 Pa for P_600, P_400 and P_200 respectively. The same effect was observed for viscosity of synthesized polyols, which decreased for all samples from 1,415; 0,790; 0,736 Pa·s to 0,359; 0,207; 0,187 Pa·s for P_600, P_400 and P_200, respectively.

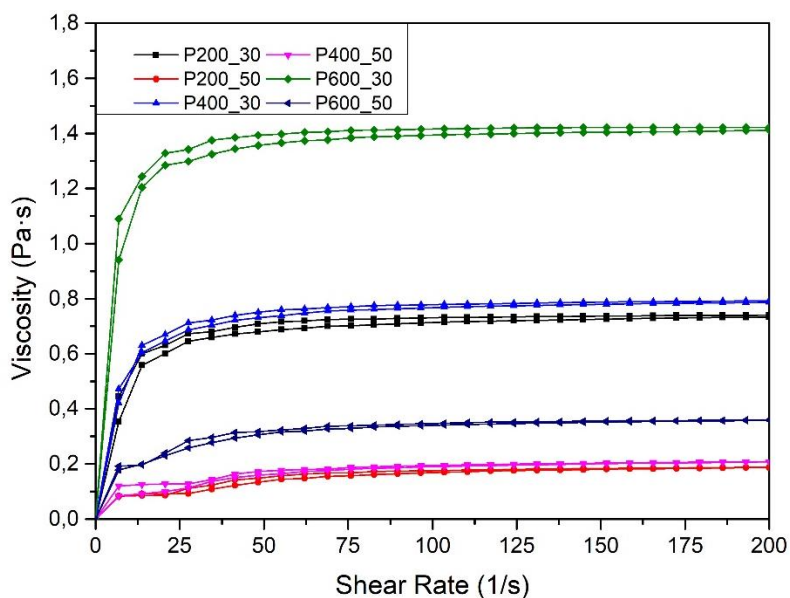


Figure 5. The viscosity curves in different temperatures of synthesized polyols

Despite the fact that the course of the curves seems to be linear (Newtonian behavior of fluid), the results analysis of the obtained by Herschel–Bulkley model shows that the flow index (n) is slightly higher than 1. This may demonstrate the shear thickening behavior of the obtained polyols³³. Moreover, the reduction of the consistency coefficient is associated with a decrease in the viscosity of the mixture. It should be noted that the Herschel–Bulkley model had the highest value of the stability index (R), which indicates a high degree of fit. Moreover, in case of all samples $\tau_0 = 0$. This means that none of the obtained prepolymers has yield stress.

Table 2. The Herschel-Bulkley linear functions for synthesized polyols

| Sample | Function | τ_0 (Pa) | μ (Pa s ⁿ) | n (-) | R |
|-------------------|-----------------------------------|---------------|----------------------------|---------|--------|
| <i>P_200_30°C</i> | $y = 0 + 0,5910 \cdot x^{1,0417}$ | 0 | 0,5910 | 1,0417 | 0,9995 |
| <i>P_200_50°C</i> | $y = 0 + 0,0802 \cdot x^{1,1624}$ | 0 | 0,0802 | 1,1624 | 0,9977 |
| <i>P_400_30°C</i> | $y = 0 + 0,6285 \cdot x^{1,0435}$ | 0 | 0,6285 | 1,0435 | 0,9997 |
| <i>P_400_50°C</i> | $y = 0 + 0,0968 \cdot x^{1,1455}$ | 0 | 0,0968 | 1,1455 | 0,9987 |
| <i>P_600_30°C</i> | $y = 0 + 1,2707 \cdot x^{1,0205}$ | 0 | 1,2707 | 1,0205 | 0,9997 |
| <i>P_600_50°C</i> | $y = 0 + 0,2243 \cdot x^{1,0900}$ | 0 | 0,2243 | 1,0900 | 0,9992 |

Where: y – shear stress; x – shear rate; τ_0 – yield stress; μ – consistency index; n – flow index; R – stability index.

3.3. Gel permeation chromatography (GPC)

The molecular weight of synthesized polyols is a crucial parameter for future application of polyurethane materials. The impact of liquefaction solvents on the molecular weight of polyols was tested by gel permeation chromatography (GPC). It should be noted that the actual values of the molecular weights may differ from the actual values. This effect has been widely described in the literature⁴⁹. For this reason, GPC was conducted only for comparison of the obtained polyols. The results of this test are presented in Table 3. The GPC curves of synthesized polyols are shown in Figure S1. in supplementary data file. The M_n of polyols was 3837; 4365; 4536 g/mol for *P_200*, *P_400*, and *P_600*, respectively. Similar results were obtained by Meng et. al.⁵⁰. It can be noticed that the average molecular weight decreases with the use of PEGs with shorter chains. The correlation between molecular weights of samples is surprising because the differences between the samples are smaller than it was predicted. It may be caused by the above-mentioned differences between the degree of conversion, reactivity and the presence of spherical hindrances⁵¹. Moreover, the polydispersity of synthesized polyols is around 1.050, indicating that their molecular weight distributions are very narrow⁵². This may be caused by long time of reaction which allowed for higher conversion degree of used substrates.

Table 3. The results of gel permeation chromatography

| Sample | M_n [g/mol] | M_w [g/mol] | PDI |
|--------------|---------------|---------------|-------|
| <i>P_200</i> | 3837 | 4049 | 1,055 |
| <i>P_400</i> | 4365 | 4555 | 1,043 |
| <i>P_600</i> | 4536 | 4793 | 1,057 |



3.4. Chemical structure characterization (FT-IR)

Fourier transform infrared spectroscopy was used for the identification of functional groups present in the synthesized polyol and is presented in Fig. 6. The curves for the substrates used are shown in Figure S2. in supplementary data file. The characteristic wide stretching vibration band of the hydroxyl groups is visible at $3150 - 3550 \text{ cm}^{-1}$. The peak located at $3000 - 2800 \text{ cm}^{-1}$ is related to the stretching vibrations of the C-H groups which are present in the CH_3 , CH_2 or CH groups. The signal in the region range of $1715 - 1750 \text{ cm}^{-1}$ is be associated with $\text{C}=\text{O}$ stretching vibration of carbonyls, which may arise from the presence of levulinians and furfurals generated during reaction of biomass chains with liquefaction solvent^{26,53}.

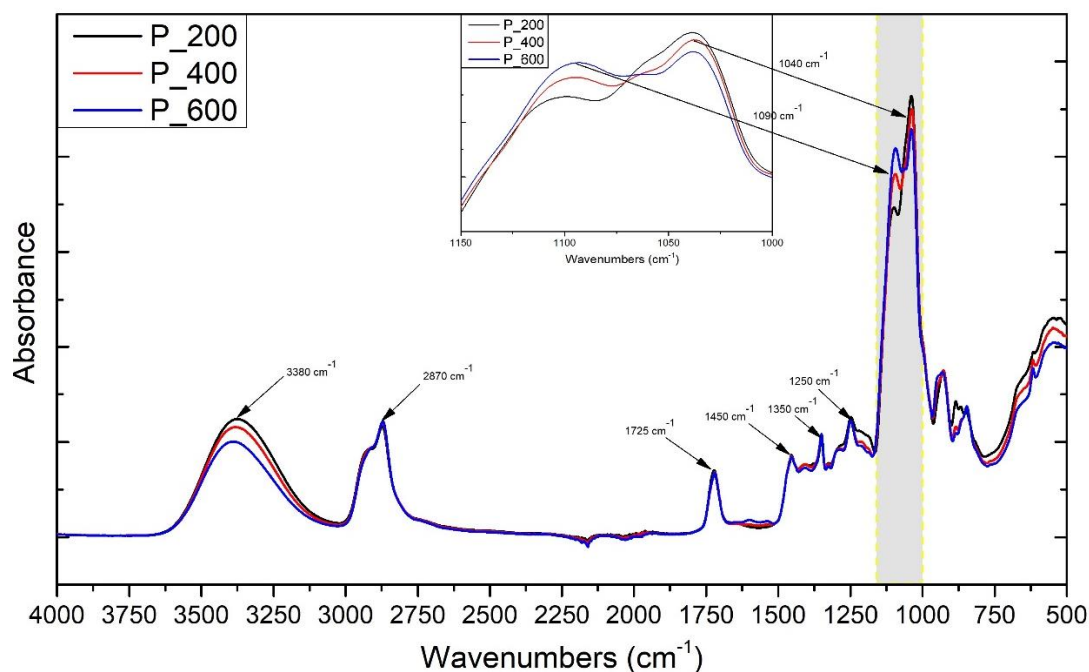


Figure 6. FT-IR spectra of polyols

The peak around 1450 cm^{-1} is associated with in-plane bending vibrations of C-H groups and and peak at 1350 cm^{-1} is associated with deformation vibrations of this groups²⁴. The absorption band around 1250 cm^{-1} may be associated with C-O-H bending vibrations of CH_2OH groups in the side chains of polyols. Moreover, C-O-C stretching vibrations may be attributed to the strong adsorption band around 1090 cm^{-1} ⁵⁴. Another strong adsorption band around 1040 cm^{-1} may be attributed to vibrations of C-O-C ether groups in structure of cellulose and its derivatives and polyethylene glycols and which suggest that obtained polyol is polyether³⁰. The main difference between the curves of synthesized polyols is noticeable at the height of the adsorption bands of the hydroxyl groups around $3150 - 3550 \text{ cm}^{-1}$, stretching vibrations of the C-O-C at 1090 cm^{-1} and vibrations of the ether groups (C-O-C) at 1040 cm^{-1} . It may be due to the use of various liquefaction solvents in each reaction mixture that caused slight changes in the structure of the polyol chains. Moreover, functional groups resulting from the analysis corresponds to the structures proposed at Fig 1. which confirms the assumed reaction course.

3.5. Thermogravimetric analysis (TGA)

As the structure of each polyurethane segments has huge impact on the thermal stability of polyurethane materials, the thermogravimetric analysis was conducted to determine the impact of liquefaction solvent molecular weight on decomposition process of synthesized polyols. Fig. 7. and Fig. 8. shows a considerable difference in weight loss and weight loss rate curves of thermal decomposition of synthesized polyols and used components. The curves of reaction mixture before liquefaction process are presented in supplementary data in Fig. S3 and Fig. S4. Moreover, the most important parameters of thermal degradation are presented in Table 4. It was considered that $T_{5\%}$ would be the best determinant of thermal stability for all substrates and products due to the presence of water particles in all substances. It was determined that lowest thermal stability has glycerol ($T_{5\%} = 135\text{ }^{\circ}\text{C}$). The degradation temperature of PEG with different molecular masses is higher and it increases from $154\text{ }^{\circ}\text{C}$; $246\text{ }^{\circ}\text{C}$; $301\text{ }^{\circ}\text{C}$ for PEG 200, PEG 400 and PEG 600, respectively. The thermal stability of polyols increases with use of polyethylene glycols with higher molecular masses and $T_{5\%}$ of polyols samples is 160 ; 169 ; $167\text{ }^{\circ}\text{C}$ for P_200, P_400 and P_600, respectively. The $T_{10\%}$ of obtained polyols is comparable, but $T_{50\%}$ is noticeable higher for samples synthesized PEG with higher molecular masses. This is due to the greater thermal stability of the polyol composed of PEG segments with longer chains.

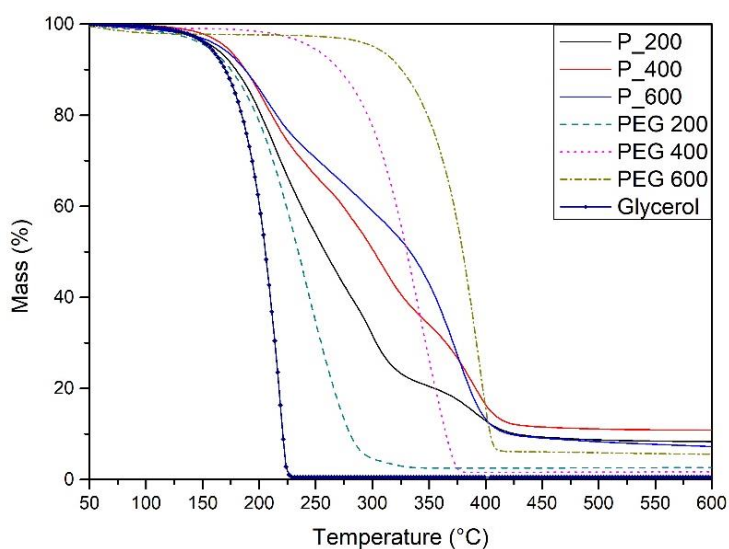


Figure 7. TGA curves of bio-based polyols and polyethylene glycols

Analyzing the thermal degradation rate of polyols and used components it can be noticed that all basic components show one step degradation, but depending of type of used PEG, obtained polyols shows two (P_200 and P_400) or three (P_600) main steps of degradation process. In addition, significant difference between thermal decomposition of mixtures before reaction and obtained polyols can be noticed. This proves that reaction between used substrates occurred. A small degradation step at temperature ca. $100\text{ }^{\circ}\text{C}$ can be assigned to presence of moisture in synthesized polyols. The first step of degradation at $T_{\max 1} = 210\text{ }^{\circ}\text{C}$ may be attributed to the degradation of glycerol and glycerol derivatives, which are present in the structure of synthesized polyols. This was confirmed by research conducted by Hejna et al.⁵⁵, where temperature of degradation of condensed glycerol was similar to obtained results. This degradation step is more noticeable for P_200 sample, as the PEG 200 degradation temperature is close to maximum of this peak ($P_{\max \text{PEG}200} = 242\text{ }^{\circ}\text{C}$). The second step of degradation

around $T_{\max 2} = 300^{\circ}\text{C}$ may be attributed to the degradation of oligomeric chains which are composed of glycerol/glycerol derivatives, PEG units, and cellulose derivatives generated during biomass liquefaction (levulinians, etc.).¹⁵ The third degradation step around $T_{\max 3} = 380^{\circ}\text{C}$ may be associated with degradation of the longest chains of PEGs chains and possible condensation products of PEG particles. This degradation step is the most noticeable for P_600 as this sample consists the highest amount of PEG with longer chains. These differences in the decomposition of synthesized polyols may influence the thermal stability of manufactured materials. We predict that materials manufactured with addition of more stable polyols will have higher thermal stability than others.

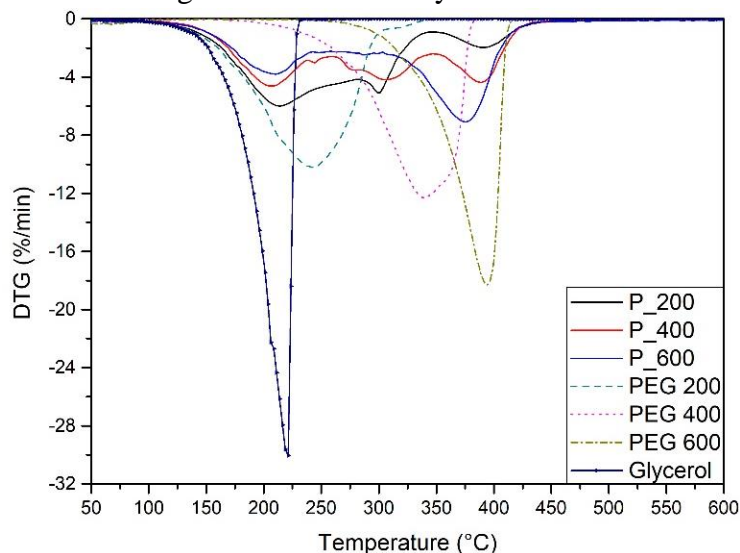


Figure 8. DTG curves of bio-based polyols and polyethylene glycols

Table 4. Results of thermogravimetric analysis of bio-based polyols

| Sample | Different % mass loss in temperature [°C] | | | $T_{\max 1}$ [°C] | $T_{\max 2}$ [°C] | $T_{\max 3}$ [°C] | Char residue after test [%] |
|-----------------|---|-----|-----|-------------------|-------------------|-------------------|-----------------------------|
| | 5% | 10% | 50% | | | | |
| <i>Glycerol</i> | 135 | 156 | 206 | 221 | - | - | 0.97 |
| <i>PEG 200</i> | 154 | 175 | 235 | 242 | - | - | 2.63 |
| <i>PEG 400</i> | 246 | 271 | 330 | 339 | - | - | 1.77 |
| <i>PEG 600</i> | 301 | 326 | 380 | 394 | - | - | 5.45 |
| <i>P_200</i> | 160 | 180 | 258 | 214 | 299 | 392 | 4.52 |
| <i>P_400</i> | 169 | 189 | 301 | 209 | 306 | 388 | 6.86 |
| <i>P_600</i> | 167 | 187 | 333 | 210 | - | 375 | 4.13 |

4. Conclusions

In this article, we have described the influence of the molecular mass of polyethylene glycols (PEGs) on the properties of the synthesized polyols. Three different polyols were synthesized by biomass liquefaction in the mixture of glycerol and PEGs with a molecular mass of 200–600 g/mol. The research conducted shows substantial differences between polyols synthesized using different liquefaction solvents.

The research shows that synthesized polyols are characterized by a hydroxyl value in the range of 589–652 mg of KOH / g, and increases with decrease of the PEG chain length. These values suggest a possible application of synthesized polyols in the manufacturing of rigid polyurethane foam. For all used PEGs, the biomass (cellulose) conversion ratio was over 90%, what indicates high efficiency of process and incorporation of biomass derivatives into the structure of the polyol. Moreover, the biomass conversion ratio is higher for samples with use of PEGs with lower molecular mass, which may prove better reactivity of shorter PEG chains with cellulose. Rheological studies showed that the viscosity of polyols increases with molecular weight of PEG. All samples were non-Newtonian fluids, which were the best fit for the Herschel–Bulkley model. The analysis of results demonstrated that all synthesized polyols show weak shear thickening behavior. Gel permeation chromatography showed that the average molecular weight of polyols decreases with the use of PEGs with shorter chains and was 3837; 4365; and 4536 g/mol for P_200, P_400, and P_600, respectively. The differences between the samples are smaller than it was predicted. This may indicate that the reaction proceeds to the moment when the final molecular weight is reached and then the process slows down. Fourier transform-infrared spectroscopy identified functional groups which are present in the synthesized polyol. These functional groups coincide with the predicted reaction products of cellulose and used liquefaction solvents. Thermogravimetric analysis of samples showed substantial differences between the decomposition processes of polyols. The thermal stability determined by T5% showed that polyols synthesized using PEGs with longer chains have higher thermal stability than others. This may have huge impact on degradation process of polyurethane materials.

The data presented here highlight the importance of the liquefaction solvent molecular weight on the properties of polyols synthesized via biomass liquefaction. Moreover, it emphasizes the importance of selecting an appropriate solvent in the biomass liquefaction process to obtain a highly valuable product, which may be used in industry. This approach may allow the biomass liquefaction process to be designed to obtain polyols with specific properties, which may be modified by amount and length of PEGs. Future studies should investigate the possible application of synthesized polyols in the manufacturing of rigid polyurethane foams or other polyurethane materials.

Conflict of interest

The authors declare that they have no conflict of interest.

Funding statement

This work was supported by The National Science Centre (NCB, Poland) in the frame of UMO-2021/43/B/ST8/02640 project— Solvothermal liquefaction as a pro-ecological method of wood-like waste management.

References

1. Ma, Y.; Xiao, Y.; Zhao, Y.; Bei, Y.; Hu, L.; Zhou, Y.; Jia, P. *React. Funct. Polym.* **2022**, *175*, 105285.
2. Beims, R. F.; Hu, Y.; Shui, H.; Xu, C. (Charles) *Biomass and Bioenergy* **2020**, *135*, 105510.
3. Jiang, W.; Kumar, A.; Adamopoulos, S. *Ind. Crops Prod.* **2018**, *124*, 325.
4. Hu, S.; Wan, C.; Li, Y. *Bioresour. Technol.* **2012**, *103*, 227.



5. Hu, S.; Li, Y. *Bioresour. Technol.* **2014**, *161*, 410.
6. Gurgel, D.; Bresolin, D.; Sayer, C.; Cardozo Filho, L.; Hermes de Araújo, P. H. *Ind. Crops Prod.* **2021**, *164*, 113377.
7. Gosz, K.; Haponiuk, J.; Piszczyk, Ł. *J. Polym. Environ.* **2018**, *26*, 3877.
8. Pantone, V.; Laurenza, A. G.; Annese, C.; Comparelli, R.; Fracassi, F.; Fini, P.; Nacci, A.; Russo, A.; Fusco, C.; D'Accolti, L. *Materials (Basel)*. **2017**, *10*.
9. Li, J.; Kuang, Y.; Bi, Y.; Sun, S.; Peng, D. *Ind. Crops Prod.* **2022**, *185*, 115112.
10. Uram, K.; Prociak, A.; Kurańska, M. *Polimery/Polymers* **2020**, *65*, 698.
11. Zemła, M.; Prociak, A.; Michałowski, S.; Cabulis, U.; Kirpluks, M.; Simakovs, K. *Int. J. Mol. Sci.* **2022**, *23*.
12. Borowicz, M.; Paciorek-Sadowska, J.; Lubczak, J.; Czupryński, B. *Polymers (Basel)*. **2019**, *11*.
13. Paciorek-Sadowska, J.; Borowicz, M.; Czupryński, B.; Tomaszewska, E.; Liszkowska, J. *Polish J. Chem. Technol.* **2018**, *20*, 24.
14. Yamada, T.; Ono, H. *Bioresour. Technol.* **1999**, *70*, 61.
15. Kosmela, P.; Hejna, A.; Formela, K.; Haponiuk, J. T.; Piszczyk, Ł. *Cellulose* **2016**, *23*, 2929.
16. da Silva, S. H. F.; Egüés, I.; Labidi, J. *Ind. Crops Prod.* **2019**, *137*, 687.
17. Gosz, K.; Kosmela, P.; Hejna, A.; Gajowiec, G.; Piszczyk, Ł. *Wood Sci. Technol.* **2018**, *52*, 599.
18. Gosz, K.; Kowalkowska-Zedler, D.; Haponiuk, J.; Piszczyk, Ł. *Wood Sci. Technol.* **2020**, *54*, 103.
19. Zhang, H.; Yang, H.; Guo, H.; Huang, C.; Xiong, L.; Chen, X. *Appl. Energy* **2014**, *113*, 1596.
20. Janiszewska, D.; Frackowiak, I.; Mytko, K. *Holzforchung* **2016**, *70*, 1135.
21. Guo, K.; Guan, Q.; Xu, J.; Tan, W. *J. Bioresour. Bioprod.* **2019**, *4*, 202.
22. Mika, L. T.; Cséfalvay, E.; Németh, Á. *Chem. Rev.* **2018**, *118*, 505.
23. Hu, S.; Luo, X.; Li, Y. *ChemSusChem* **2014**, *7*, 66.
24. Zhang, J.; Hori, N.; Takemura, A. *Ind. Crops Prod.* **2019**, *138*, 111455.
25. Wang, H.; Chen, H. Z. *J. Chinese Inst. Chem. Eng.* **2007**, *38*, 95.
26. Braz, A.; Mateus, M. M.; dos Santos, R. G.; Machado, R.; Bordado, J. M.; Correia, M. J. N. *Biomass and Bioenergy* **2019**, *120*, 200.
27. Mun, S. P.; Hassan, E. B. M. *J. Ind. Eng. Chem.* **2004**, *10*, 473.
28. Maldas, D.; Shiraishi, N. *Polym. Plast. Technol. Eng.* **1996**, *35*, 917.
29. Yona, A. M. C.; Budija, F.; Kričej, B.; Kutnar, A.; Pavlič, M.; Pori, P.; Tavzes, Č.; Petrič, M. *Ind. Crops Prod.* **2014**, *54*, 296.
30. Briones, R.; Serrano, L.; Llano-Ponte, R.; Labidi, J. *Chem. Eng. J.* **2011**.
31. Hejna, A.; Kosmela, P.; Klein, M.; Formela, K.; Kopczyńska, M.; Haponiuk, J.; Piszczyk, Ł. *J. Polym. Environ.* **2018**, *26*, 3334.
32. Kosmela, P.; Kazimierski, P.; Formela, K.; Haponiuk, J.; Piszczyk, Ł. *J. Ind. Eng. Chem.* **2017**, *56*, 399.
33. Huang, X.; De Hoop, C. F.; Xie, J.; Wu, Q.; Boldor, D.; Qi, J. *Mater. Des.* **2018**, *138*, 11.
34. Chen, L.; Pan, Z.; Hu, G. *-H AIChE J.* **1993**, *39*, 1455.
35. Li, T. T.; Feng, L. F.; Gu, X. P.; Zhang, C. L.; Wang, P.; Hu, G. H. *Ind. Eng. Chem. Res.* **2021**, *60*, 2791.
36. Ha Tran, M.; Lee, E. Y. *J. Ind. Eng. Chem.* **2020**, *81*, 167.
37. Chang, C.; Liu, L.; Li, P.; Xu, G.; Xu, C. *Ind. Crops Prod.* **2021**, *160*, 113098.
38. Juhaida, M. F.; Paridah, M. T.; Mohd. Hilmi, M.; Sarani, Z.; Jalaluddin, H.; Mohamad Zaki, A. R. *Bioresour. Technol.* **2010**, *101*, 1355.
39. Zhao, H.; Gao, W. C.; Li, Q.; Khan, M. R.; Hu, G. H.; Liu, Y.; Wu, W.; Huang, C. X.; Li, R. K. Y. *Adv. Colloid Interface Sci.* **2022**, *303*, 102644.
40. Gao, W. C.; Wu, W.; Chen, C. Z.; Zhao, H.; Liu, Y.; Li, Q.; Huang, C. X.; Hu, G. H.; Wang, S. F.; Shi, D.; Zhang, Q. C. *ACS Appl. Mater. Interfaces* **2022**, *14*, 1874.
41. Xu, W.; Zhang, R.; Liu, W.; Zhu, J.; Dong, X.; Guo, H.; Hu, G. H. *Macromolecules* **2016**, *49*, 5931.
42. Olszewski, A.; Nowak, P.; Kosmela, P.; Piszczyk, Ł. **2021**.
43. Olszewski, A.; Kosmela, P.; Mielewczyk-Gryń, A.; Piszczyk, Ł. *Materials (Basel)*. **2020**, *13*, 2028.



44. Olszewski, A.; Kosmela, P.; Piszczyk, Ł. *Eur. J. Wood Wood Prod.* **2022**, *80*, 57.
45. Olszewski, A.; Kosmela, P.; Piszczyk, Ł. *Eur. J. Wood Wood Prod.* **2022**, *80*, 57.
46. Jiang, K.; Chen, W.; Liu, X.; Wang, Y.; Han, D.; Zhang, Q. *Eur. Polym. J.* **2022**, *179*, 111572.
47. Budarin, V. L.; Clark, J. H.; Lanigan, B. A.; Shuttleworth, P.; Macquarrie, D. J. *Bioresour. Technol.* **2010**, *101*, 3776.
48. Głowińska, E.; Datta, J. *Ind. Crops Prod.* **2014**, *60*, 123.
49. Mohd Noor, M. A.; Sendjarevic, V.; Abu Hassan, H.; Sendjarevic, I.; Tuan Ismail, T. N. M.; Seng Soi, H.; Hanzah, N.; Ghazali, R. *J. Appl. Polym. Sci.* **2015**, *132*, 1.
50. Meng, F.; Zhang, X.; Yu, W.; Zhang, Y. *Ind. Crops Prod.* **2019**, *137*, 377.
51. Feng, L. F.; Hu, G. H. *AIChE J.* **2004**, *50*, 2604.
52. Chang, C.; Feng, L.-F.; Gu, X.-P.; Zhang, C.-L.; Chen, X.; Hu, G.-H. *AIChE J.* **2022**, *68*, e17572.
53. Amado, M.; Bastos, D.; Gaspar, D.; Matos, S.; Vieira, S.; Bordado, J. M.; Galhano dos Santos, R. *J. Clean. Prod.* **2021**, *304*.
54. Grilc, M.; Likožar, B.; Levec, J. *Biomass and Bioenergy* **2014**, *63*, 300.
55. Hejna, A.; Kosmela, P.; Klein, M.; Gosz, K.; Formela, K.; Haponiuk, J.; Piszczyk, Ł. *Polym. Degrad. Stab.* **2018**, *152*, 29.

